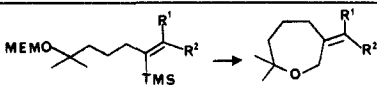
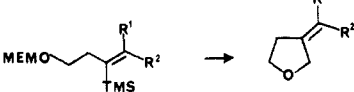
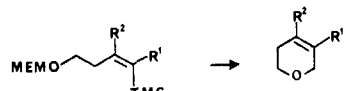


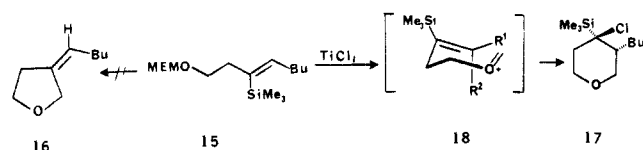
Table I. Acetal-Vinylsilane Cyclizations

entry	conversion	reactn condtn ^a	yield, % ^b	stereo-chem ^c
1		-15 °C, 12 h	71	>98% Z
2	R ¹ = H, R ² = <i>n</i> -Bu R ¹ = <i>n</i> -Bu, R ² = H (12)	-15 °C, 24 h	57	>98% E
3		-5 °C, 12 h	81	97% E
4	(13) R ¹ = <i>n</i> -Bu, R ² = H (14)	-10 °C, 6 h	86	~60% Z ^d
5	R ¹ = Et, R ² = <i>n</i> -Bu R ¹ = <i>n</i> -Bu, R ² = Et	-10 °C, 6 h	89	~60% Z ^d
6		-60 °C, 2 h ^e	78	
7	R ¹ = Br, R ² = H	-20 °C, 2 h ^f	83	
8	R ¹ = (CH ₂) ₃ Ph, R ² = H	-20 °C, 1 h	71	
9	R ¹ = R ² = H R ¹ = H, R ² = Me	-20 °C, 1 h	65	

^a In CH₂Cl₂ (substrate concentration = 0.03–0.05 M). The catalyst was SnCl₄ (distilled from P₂O₅ and stored under argon) unless otherwise noted. The equivalents of catalyst were not optimized: 2 equiv were employed for entries 1 and 2, and 5 equiv for entries 3–5, 8, and 9. ^b Reference 12. ^c By capillary GC analysis except for entries 4 and 5 which were determined from the 250-MHz ¹H NMR spectrum of the crude product. ^d The origin of the lack of stereospecificity in these cases will be discussed in a subsequent full account of this work. ^e TiCl₄ (3 equiv, freshly distilled from Cu powder) was employed. ^f TiCl₃ (O-*i*-Pr) (3 equiv) was employed.

preparation of the 3- and 4-substituted 5,6-dihydro-2*H*-pyrans (entries 6–9) demonstrates the success of acetal-vinylsilane cyclizations that are also endocyclic⁹ with respect to the vinylsilane terminator.

In marked contrast to the successful preparation of the (*E*)-alkylidenetetrahydrofuran **14** (entry 3), cyclization of the (*Z*)-vinylsilane acetal **15** with TiCl₄ did not afford **16** but gave almost exclusively tetrahydropyran **17**.^{12,18–20} The conversion of **15** →



17 was quite rapid and occurred readily at -55 °C (2 h, 81% yield of **17**). The observation that the stereochemistry of an alkene can completely control whether a cyclization reaction occurs in an endo- or exocyclic sense with respect to this component is, to our knowledge, without precedent. We rationalize this startling observation by suggesting that the rate of cyclization to form the five-membered product is insensitive to the stereochemistry at the alkene terminus, while the rate of cyclization to form the six-membered product is highly dependent on the orientation of the terminal substituent. Specifically, cyclization of **15** → **17** is facile since the butyl group would adopt a favored quasi-equatorial orientation in a chairlike^{7a} cyclization transition state **18** (R¹ = *n*-Bu), while the similar mode of cyclization of substrates with an (*E*)-vinylsilane substituent (entries 3–5) is disfavored since an alkyl group would occupy a quasi-axial position (**18**, R² = alkyl).²¹

In summary, acetal-vinylsilane cyclizations should prove to be a useful addition to the methods currently available for preparing five-, six-, and seven-membered ring oxygen heterocycles. These

cyclization reactions provide the first route for preparing 3-alkylidene oxacyclics in a stereocontrolled fashion.

Acknowledgment. This study was supported by PHS Grant GM-30859. NMR and mass spectra were determined with spectrometers purchased with the assistance of NSF Departmental Instrumentation Grants.

Supplementary Material Available: Full experimental details and characterization data for the preparation of **10**, **11**, and **17** (4 pages). Ordering information is given on any current masthead page.

The Taylor Vortex: The Measurement of Viscosity in NMR Samples

Marisol Vera[†] and John B. Grutzner*

Department of Chemistry, Purdue University
West Lafayette, Indiana 47907

Received November 8, 1985

Nuclear relaxation, molecular motion, and solution viscosity are intimately linked through hydrodynamic models.^{1–3} NMR *T*₁ relaxation times provide detailed information about molecular properties.^{4–6} In this paper a method for measuring viscosity in NMR samples is introduced. NMR images of coherent periodic flow are presented.

The transition from laminar to turbulent flow is specified by the Reynolds number—a function of viscosity. That such a transition generates cyclic vortices has been known since ancient times.⁷ In his classic 1923 paper, Taylor⁸ established the con-

[†] National Hispanic Scholarship Fund recipient 1984.

(1) Bloembergen, N.; Purcell, E. M.; Pound, R. V. *Phys. Rev.* **1948**, *73*, 679.

(2) Boere, R. T.; Kidd, G. *Ann. Rep. NMR Spectrosc.* **1982**, *12*, 319.

(3) Bauer, D. R.; Brauman, J. I.; Pecora, R. J. *Am. Chem. Soc.* **1974**, *96*, 6840.

(4) Jonas, J. *Acc. Chem. Res.* **1984**, *17*, 74; *Science (Washington, D.C.)* **1982**, *216*, 1176.

(5) Lyerla, J. R.; Levy, G. C. *Top. Carbon-13 NMR Spectrosc.* **1974**, *1*, 79.

(6) (a) Kratochwill, A. *Nucl. Magn. Reson.* **1983**, *12*, 96. (b) Koch, W.; Weingartner, H. *Ibid.* **1984**, *13*, 110 and previous reviews in this series.

(18) The tetrahydropyran structure of **17** is firmly based on fully decoupled ¹H and ¹³C NMR spectra (see supplementary material). Alternate tetrahydrofuran structures [e.g., 3-(trimethylsilyl)-3-(bromochloromethyl)tetrahydrofuran] are rigorously excluded.

(19) This and other examples²⁰ suggest that the energy difference between a β-silyl secondary cation and an α-silyl tertiary cation may be small.

(20) Mikami, H.; Kishi, H.; Nakai, T. *Tetrahedron Lett.* **1983**, *24*, 795.

(21) We suggest that a terminal substituent which is cis to the connecting atoms of a nascent ring should in general disfavor cyclization in an endocyclic sense as a result of the steric interactions between this substituent and the forming ring.^{7a}

ditions for vortex development between concentric cylinders. The phenomenon (Taylor vortex flow; TVF) has been a paradigm for studies in fluid dynamics.^{9,10}

The Taylor Vortex. When a liquid is contained within the annulus between two concentric cylinders and the inner tube rotated, a wide variety of fluid motions develop.⁹ At low rotational speeds the azimuthal velocity profile, $V(r)$ (cm/s), for Couette flow is given by

$$V(r) = 2\pi F(-q^2 r + a^2/r)/(1 - q^2)$$

where a and b (cm) are the radii of the inner and outer cylinders respectively, F (Hz) is the angular frequency of the inner tube, $q = a/b$ and $d = b - a$.

At higher speeds a critical transition occurs to a new fluid motion—TVF.^{8,9} A dimensionless Taylor number characterizes the flow

$$T = [4q/(1 + q)][R^2(d/a)] \quad (1)$$

R is the Reynolds Number defined as $R = 2\pi Fad/\nu$, where ν (cm²/s) is the kinematic viscosity of the liquid (viscosity/density). The liquid column breaks into discrete cells with periodic horizontal boundaries whose separation equals the annular gap.^{8,9} Coherent liquid circulation in the vertical plane is given by^{2,10}

$$V_z = \sum_{k=0}^{\infty} h_k \sin \frac{2\pi kz}{\lambda}$$

where λ is the cell length $\approx d$. Viscosity measurement is accomplished by measuring the spinning frequency for the onset of TVF [F_c (Hz)]. Rearrangement of eq 1 gives

$$\nu = 2\pi F_c ad [4d/T_c(a + b)]^{1/2} \quad (2)$$

where T_c is the critical Taylor number. T_c has been established theoretically^{8,11} and experimentally¹² and the Di Prima¹¹ results are described as

$$T_c q^2 = 502.00 + 1358.1q + 1415.3q^2 + 114.81q^3$$

The viscosity ranges that are accessible with standard NMR tubes at obtainable spinning speeds on a standard spectrometer are given in supplementary material.

Spinning Sidebands and Coherent Motion. An NMR sample spinning uniformly in a static transverse magnetic field gradient generates a sideband modulation pattern with peaks separated by the spinning frequency (F).¹³ The nuclei must move periodically across a field gradient in order to develop the coherence necessary for sideband generation. In a transverse gradient under Couette flow conditions, with the inner tube spinning (below F_c) and the outer tube fixed, the liquid in the inner tube gives a standard sideband pattern with spacing F , whereas the liquid in the annulus shows no detectable splitting (Figure 1). All azimuthal velocities between F at the inner wall and zero at the outer wall exist in Couette flow. Thus spinning sidebands will be generated at all frequencies. They are superimposed and so discrete frequencies are not expected. In an axial gradient no sidebands are generated as there is no coherent vertical motion.

When the inner tube speed is increased above F_c a major spectral change is observed. Rotating liquid cores intersect the axial gradient and are detectable as a sideband pattern which images the TVF (Figure 2). TVF generates coherent vertical motion in each cell which gives rise to cell sideband patterns. Each cell has its centerband, and this series of centerbands produces the series of intense peaks observed in Figure 2. The uniform vertical spacing of Taylor vortex cells is reflected in the uniform spacing of the centerband peaks. Peak separation is directly proportional to the strength of the axial gradient (supplementary

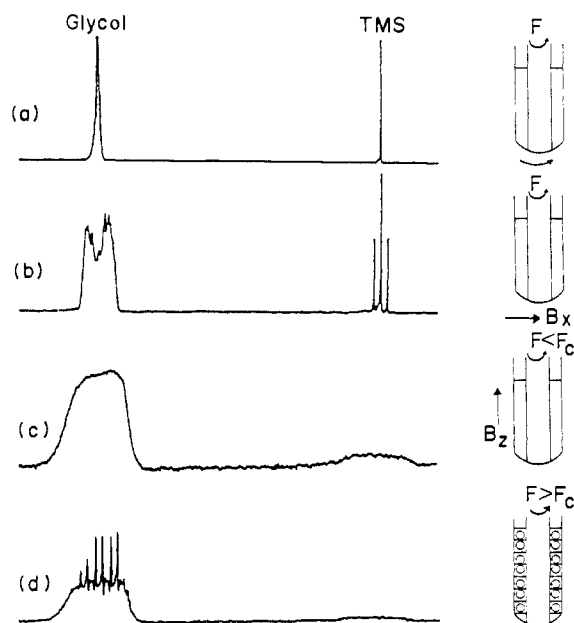


Figure 1. Proton-decoupled 50-MHz ¹³C spectra of Me₄Si (5-mm tube) and ethylene glycol (annulus of 10-mm tube). (a) Both tubes spinning at $F = 20$ Hz in a uniform magnetic field; (b) inner tube spinning at 20 Hz in a transverse gradient ($B_x \sim 3$ mT/m); (c) inner tube spinning at 20 Hz in an axial gradient ($B_z \sim 2$ mT/m); (d) same as (c) with $F = 40$ Hz. Coherent TVF gives peak pattern in (d).

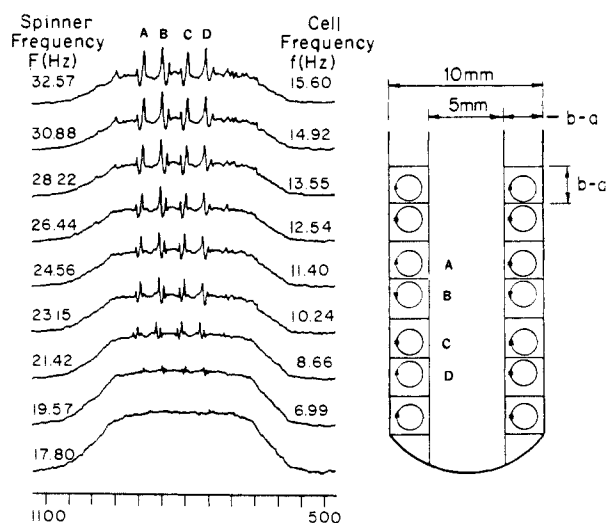


Figure 2. Viscosity measurement of ethylene glycol/D₂O (80:20 v/v) from detection of onset of TVF as function of inner tube spinning speed. $F_c \approx 18$ Hz. NMR as for Figure 1. $B_z \sim 2$ mT/m. Peaks labeled A–D are the centerband from each cell—see inset. Cell spinning frequency [f (Hz)] is shown.

material). Furthermore, each centerband is flanked by a series of spinning sidebands—usually of lower intensity. The sideband spacing is independent of the field gradient but increases with increasing F . The cell sideband frequency (f) measures the spiral frequency of the Taylor vortex core in the vertical plane. The intensity of the pattern increases as the spinning frequency is increased. Taylor vortex motion is thus coherent at the molecular level. The measurement of viscosity is accomplished by the measurement of the frequency of onset of the Taylor vortex.

Measurement of Viscosity. The simplest method for determining F_c is the detection of the sideband onset pattern as shown in Figure 2. This method gives limited precision as the distinction of the weak sideband pattern from the strong background signal and noise is quite subjective. A plot of f vs. F suggests a convenient alternative. The curve follows the empirical relationship

$$\ln(F) = \ln(F_c) + kf^2 \quad (3)$$

(7) Ecclesiastes, Chapter One.

(8) Taylor, G. I. *Philos. Trans. R. Soc. London, A* **1923**, 223, 289.

(9) For a comprehensive review, see: Di Prima, R. C.; Swinney, H. L. *Top. Appl. Phys.* **1981**, 45, 139.

(10) Marcus, P. S. *J. Fluid Mech.* **1984**, 146, 65.

(11) Walowit, J.; Tsao, S.; Di Prima, R. C. *Appl. Mech.* **1964**, 31, 585.

(12) Cole, J. A. *J. Fluid Mech.* **1976**, 75, 1 and references therein.

(13) Williams, G. A.; Gutowsky, H. S. *Phys. Rev.* **1956**, 104, 278.

Table I. NMR Viscosity Determination

sample	T , °C	F_c , Hz	ν_{NMR} , ^c cSt	ν_{Ubb} , ^d cSt
EG ^a	23	32.62 ± 0.2	14.85	14.57 ± 0.09
EG/D ₂ O (80:20 v/v)	23.5-23.8	17.55 ± 0.26	7.98	7.84 ± 0.10
EG/CH ₃ CN (80:20v:v)	23.0 ± 0.5 ^b	11.21 ± 0.25	5.10	5.16 ± 0.01
Carbowax 600/ Me ₂ SO (20% w/w)	34.0 ± 0.5 ^b	15.23 ± 0.25	6.93	6.94 ± 0.12
		15.27 ± 0.25	6.95	

^aEG = ethylene glycol. ^bActual temperature calculated with a C-13 thermometer insert (acetone-*d*₆/CCl₄; 1:1 v/v). Led, J. L.; Petersen, S. G. *J. Magn. Reson.* 1978, 32, 1. ^c $\nu_{\text{NMR}} = F_c/219.7$ (Stokes) for 5-mm o.d./NMR tube inside 10-mm tube. $a = 0.24765$ cm, $b = 0.45085$ cm, $q = 0.5493$, $T_c = 5614.5$. ^dViscosity measured with Ubbelohde viscometer.

where k is an arbitrary constant. The intercept of this linear plot gives F_c . Substitution of F_c into eq 2 gives the kinematic viscosity of the liquid. The results obtained for several test liquids are shown in Table I. Viscosities determined by using a conventional Ubbelohde viscometer and the NMR values agree within 2%. The experiment is independent of the choice of nucleus. Both homonuclear and heteronuclear measurements are feasible provided peak separation is larger than the gradient width. Individual components in a mixture give the same viscosity as the fluid flow is governed by the bulk viscosity (cf. Carbowax 600/Me₂SO mixture).

An implication of the current work is that an NMR image of coherent linear flow should be detectable in a rotating magnetic field.

Acknowledgment. The generous financial support of Eli Lilly & Co. is gratefully acknowledged. M. Vera was supported by a Committee on Institutional Cooperation (CIC) Minority fellowship. The continued instrumental expertise of Dr. R. Santini is gratefully acknowledged.

Supplementary Material Available: NMR image of TVF in ethylene glycol as a function of axial field gradient strength and a table of a , b , d , q , T , F_c/ν , and ν values (3 pages). Ordering information is given on any current masthead page.

Intramolecular [4 + 2] Cycloadditions of Nitroalkenes with Olefins[†]

Scott E. Denmark,^{*1a} Michael S. Dappen,^{1b} and Christopher J. Cramer^{1c}

Roger Adams Laboratory, School of Chemical Sciences
University of Illinois, Urbana, Illinois 61801

Received October 1, 1985

As part of a program aimed at the development of general methods of construction of polycyclic ring systems, we have been investigating the intramolecular cycloadditions of various heterodienes with olefins.² Our efforts have focused on the N=O family of heterodienes shown in Chart I. We have recently reported successful cycloadditions with nitrosoalkenes^{3,4} and

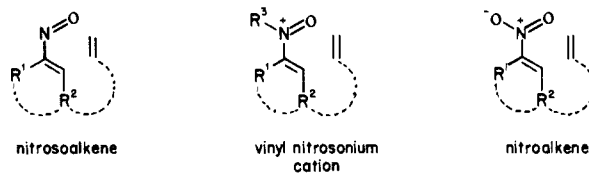
[†] Dedicated to Professor Dr. Albert Eschenmoser on the occasion of his 60th birthday.

(1) (a) Fellow of the Alfred P. Sloan Foundation (1985-1987), NSF Presidential Young Investigator (1985-1990). (b) Taken in part from: Dappen, M. S. Ph.D. Thesis, University of Illinois, Urbana, 1985. (c) NSF Graduate Fellow, 1984-1987.

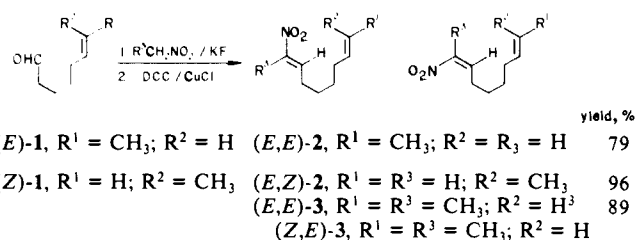
(2) For reviews of heterodiene [4 + 2] cycloadditions, see: (a) Desimoni, G.; Tacconi, G. *Chem. Rev.* 1975, 75, 651. (b) Schmidt, R. R. *Angew. Chem., Int. Ed. Engl.* 1973, 12, 212. For intramolecular [4 + 2] cycloadditions, see: Ciganek, E. *Org. React.* 1984, 32, 1.

(3) Denmark, S. E.; Dappen, M. S.; Sternberg, J. A. *J. Org. Chem.* 1984, 49, 4741.

Chart I



Scheme I



Scheme II

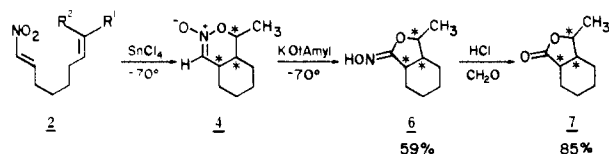


Table I. Cycloadditions of Nitroalkenes 2 and 3^{a,b}

substrate	solvent	temp, °C	time, h	trans	cis	yield, ^c %
(<i>E,E</i>)-2	CH ₂ Cl ₂	-70	2.25	52	48	59
(<i>E,Z</i>)-2	CH ₂ Cl ₂	-70	2.25	75	25	68
(<i>E,E</i>)-3 ^d	toluene	-29 → 0	3	>98	<2	80 ^e
(<i>Z,E</i>)-3 ^f	toluene	-78	7	<2	>98	63

^aNitroalkene was 0.04 M and 1.0-1.6 equiv of SnCl₄ were used. Best yields were obtained with fresh nitroalkene. ^bCis/trans product ratios were determined by ¹H NMR and GC as described in the text for 4 and 5. ^cYields for isolated, purified nitronates. ^d>98% *E* by ¹H NMR. ^e11% of *i* was isolated in this run. ^f>98% *Z* by ¹H NMR.

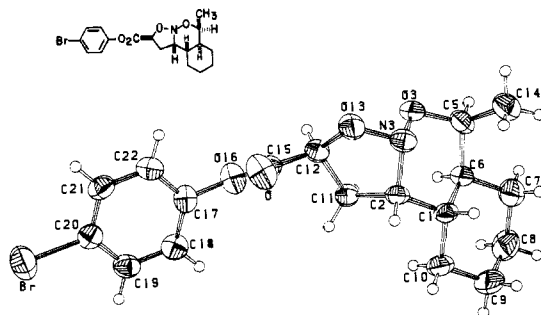


Figure 1. ORTEP plot of double cycloadduct (35% probability).

vinylnitrosonium cations.^{4b} In this paper we wish to report that nitroalkenes also serve admirably as 4 π components in highly stereoselective cycloadditions with unactivated alkenes.⁵

(4) (a) Denmark, S. E.; Dappen, M. S.; Sternberg, J. A. "Abstracts of Papers", 187th American Chemical Society Meeting, St. Louis, MO, April 1984; American Chemical Society: Washington, DC, 1984; ORGN 45. (b) Denmark, S. E.; Cramer, C. J. "Abstracts of Papers", 189th American Chemical Society Meeting, Miami, FL, April 1985; American Chemical Society: Washington, DC, 1985; ORGN 151.